Hydrogen-induced suppression of the peritectoid reaction of alpha -Pd+Pd_3Gd (or H-Pd_5RE (RE identical to Sm or Eu)) to Pd_7RE (RE identical to Gd, Sm or Eu)

1994 J. Phys.: Condens. Matter 6 2321

(http://iopscience.iop.org/0953-8984/6/12/005)

J. Phys.: Condens. Matter 6 (1994) 2321–2334. Printed in the UK

Hydrogen-induced suppression of the peritectoid reaction of α-Pd + Pd_3Gd (or H-Pd_5RE (RE ≡ Sm or Eu)) to Pd_7RE (RE ≡ Gd, Sm or Eu)

Y Sakamoto†, K Takao† and T B Flanagan‡

† Department of Materials Science and Engineering, Nagasaki University, Nagasaki 852, Japan

‡ Department of Chemistry, The University of Vermont, Burlington, VT 05405-0125, USA

Received 19 October 1993

Abstract. The peritectoid reaction of α-Pd + Pd_3Gd (or H-Pd_5RE (RE ≡ Sm or Eu)) to Pd_7RE (RE ≡ Gd, Sm or Eu) in Pd–Gd, Pd–Sm and Pd–Eu alloys is found to be suppressed after the slow cooling to room temperature of alloys in the presence of hydrogen (about 30 bar) which has been introduced above the peritectoid reaction temperature and then maintained during slow cooling. The suppression of the ordering to the Pd_7Gd ordered structure in Pd–Gd alloys is believed to be due to the retardation of nucleation and growth of the Pd_7Gd ordered domain during cooling as a consequence of a weakening of Pd–Gd bonding by the dissolved hydrogen in the α-Pd phase. In the cases of Pd–Sm and Pd–Eu alloys, the suppression is related to the transition of H-Pd_5Sm(Eu) phases which initially coexist with α-Pd phases to $L1_2$-type Pd_3Sm(Eu) phases under hydrogen exposure. The initially short-range-ordered Pd_7Gd (Sm, Eu) phases coexist with the α-Pd, Pd_3Gd or H-Pd_5Sm(Eu) phases below the peritectoid reaction temperatures, but relatively at high temperatures they also have a tendency to disorder upon hydrogen exposure. Similarly, for the low-temperature hydrogen treatments, the initially coexisting H-Pd_5Sm(Eu) phases with the Pd_7Sm(Eu) phases also transform to the $L1_2$-type Pd_3Sm(Eu) phases. The Pd_3Sm(Eu) phases which have been transformed by hydrogen are reverse transformed into the α-Pd and H-Pd_5Sm(Eu) phases by heating above the peritectoid reaction temperatures via the formation of Pd_7Sm(Eu) phases.

1. Introduction

The formation of the ordered Pd_7RE (RE ≡ Gd [1], Sm [2], or Eu [3]) phase, which is a Pt_7Cu-type superlattice [4], has been found to be accompanied by a peritectoid reaction: α-Pd + $L1_2$-type Pd_3Gd (or H-Pd_5RE (RE ≡ Sm, or Eu)†) ↔ Pd_7RE in the Pd–RE alloys. In the more hypoperitectoid alloys, the order–disorder transitions of α-Pd ↔ Pd_7RE correspond to the solid solubility limit of the solute metals.

It has been shown recently [5] that the phase transition of the α-Pd solid solution to the corresponding ordered Pd_7RE (RE ≡ Gd or Sm) and/or Pd_7Li phases in the Pd–10.0 at.% Gd, Pd–6.5 at.% Sm, Pd–8.0 at.% Sm and Pd–7.2 at.% Li alloys is suppressed by exposure to hydrogen at pressures of 20 bar and by subsequent slow cooling to room temperature with the pressure maintained. Furthermore, it has been observed that, even in the cases of the alloys initially consisting of two phases, α-Pd and Pd_7RE (RE ≡ Gd, or Sm) and/or Pd_7Li phases below the solid solubility limits of the solute metals but at relatively high

† The designation H-Pd_5RE does not refer to hydrogen in Pd_5RE but rather is a crystallographic designation for the structure [12].

0953-8984/94/122321+14$19.50

temperatures within the two-phase regions, the ordered Pd_7RE and Pd_7Li phases have a tendency to disorder upon exposure to hydrogen (above 20 bar) and to remain disordered during subsequent slow cooling in hydrogen (above 20 bar).

The suppression effect of ordering to Pd_7RE (RE ≡ Gd or Sm) and/or Pd_7Li structures is suggested to be due to the retardation of nucleation and growth of the ordered domain during cooling as a consequence of weakening of the Pd–RE and/or Pd–Li bonds by the dissolved hydrogen.

Salomons *et al* [6] and Doyle *et al* [7] have also suggested hydrogen suppression effects of ordering as judged from measurements of hydrogen solubilities in $Pd_{91}Y_9$ [6] and Pd–8 at.% Y [7] alloys. Their suggestions of hydrogen-suppressed ordering as based on indirect evidence have been confirmed directly in our work using electron diffraction [5].

The purpose of the present work is to examine the effect of hydrogen exposure on the peritectoid reaction of α-Pd + Pd_3Gd (or H-Pd_5RE (RE ≡ Sm or Eu)) to Pd_7RE (RE ≡ Gd, Sm or Eu).

The Pd_7RE structure is a derivative of the $L1_2$-type Pd_3 RE phase [8, 9]; in the structure, triangularly stacked layers of Pd_3RE alternate with triangularly stacked layers of palladium on a (111) plane in an FCC lattice. As has been previously reported for H-Pd_5RE (RE ≡ Sm [2] or Eu [3]), the H-Pd_5RE phase does not have a simple crystal structure of a hexagonal $CaCu_5$-type unit cell [10, 11] because there are some discrepancies between the experimental x-ray diffraction peak positions and those simulated by assuming the same crystal structure of a hexagonal $CaCu_5$ [10, 11]. The crystal structure of H-Pd_5RE (RE ≡ Sm or Eu) is also considered to have a two- or three-block structure, the H-Pd_5Ce [12, 13] phase, in which each block is composed of two $CaCu_5$-type layers of hexagonal symmetry [14, 15].

2. Experimental details

The alloy samples were prepared as previously described [1–3]. The compositions used in this study are Pd–11.5 at.% Gd, Pd–14.0 at.% Gd, Pd–11.5 at.% Sm, Pd–13.7 at.% Sm, Pd–10.0 at.% Eu, Pd–11.2 at.% Eu, Pd–12.2 at.% Eu, Pd–13.3 at.% Eu and Pd–14.3 at.% Eu alloys. After a homogenizing anneal, the arc-melted alloy buttons were cut with a microcutter into samples which were used for electron microscopy observation, x-ray diffraction and electrical resistance measurements, and their surfaces were abraded with emery paper. The sample thicknesses were about 200 μm.

Before hydrogen exposure, all the samples were annealed *in vacuo* by cooling from about 1123 K to room temperature at 50 K h^{-1}. Hydrogen exposure under a pressure of 30 bar was carried out in a Hastelloy tube vessel. According to the previously determined Pd-rich side phase diagrams of the Pd–Gd [1], Pd–Sm [2] and Pd–Eu [3] systems, the temperatures for hydrogen exposure treatments were chosen to correspond to two-phase regions of α-Pd + Pd_3Gd, and of α-Pd + H-Pd_5RE (RE ≡ Sm and Eu), i.e. above the peritectoid temperatures. Hydrogen exposure of some samples was also carried out at specified temperatures below the peritectoid temperatures, i.e. in the two-phase regions α-Pd + Pd_7Gd, Pd_7Gd + Pd_3Gd, α-Pd + $Pd_7Sm(Eu)$ and $Pd_7Sm(Eu)$ + H-$Pd_5Sm(Eu)$. The hydrogen exposure temperatures employed for these alloys are shown in the partial phase diagrams [1–3] in figures 1–3.

After evacuation of the annealed samples at the specified temperatures (figures 1–3), the samples, which were employed for electron microscopy, x-ray diffraction and electrical resistance measurements, were exposed to a hydrogen pressure of 30 bar, held at the specified temperatures for 1 h and then cooled to room temperature at a rate of 50 K h^{-1} unless specified otherwise, while the pressure was maintained.

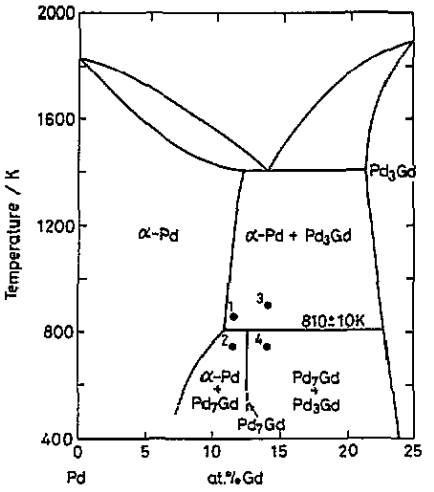

Figure 1. Partial phase diagram of the Pd–Gd system [1]. The temperatures for hydrogen exposure of the alloys were as follows: point 1, 863 K for Pd–11.5 at.% Gd; point 2, 753 K for Pd–11.5 at.% Gd; point 3, 903 K for Pd–14.0 at.% Gd; point 4, 753 K for Pd–14.0 at.% Gd.

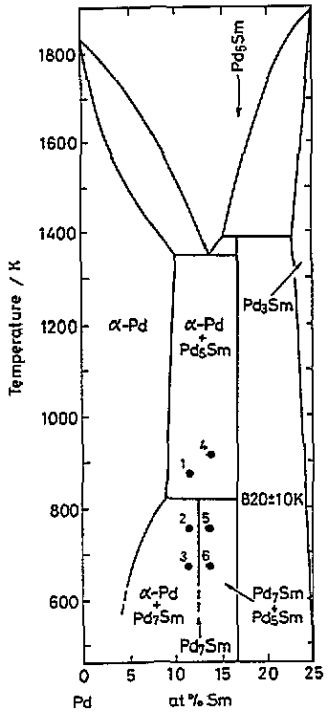

Figure 2. Partial phase diagram of the Pd–Sm system [2]. The temperatures for hydrogen exposure of the alloys were as follows: point 1, 873 K for Pd–11.5 at.% Sm; point 2, 753 K for Pd–11.5 at.% Sm; point 3, 673 K for Pd–11.5 at.% Sm; point 4, 913 K for Pd–13.7 at.% Sm; point 5, 753 K for Pd–13.7 at.% Sm; point 6, 673 K for Pd–13.7 at.% Sm.

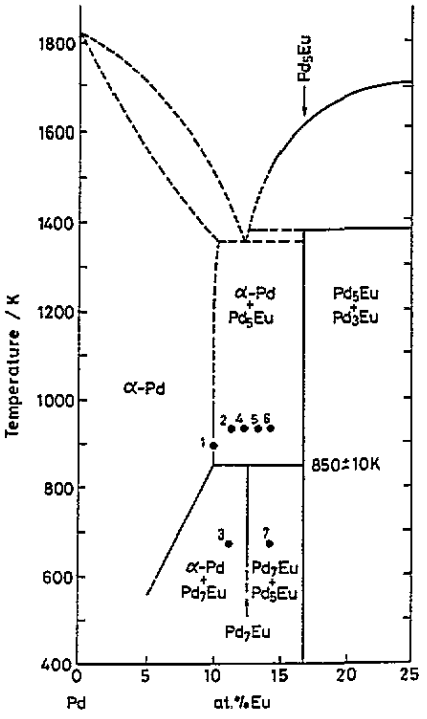

Figure 3. Partial phase diagram of the Pd–Eu system [3]. The temperatures for hydrogen exposure of the alloys were as follows: point 1, 893 K for Pd–10.0 at.% Eu; point 2, 933 K for Pd–11.2 at.% Eu; point 3, 673 K for Pd–11.2 at.% Eu; point 4, 933 K for Pd–12.2 at.% Eu; point 5, 933 K for Pd–13.3 at.% Eu; point 6, 933 K for Pd–14.3 at.% Eu; point 7, 673 K for Pd–14.3 at.% Eu.

3. Results and discussion

3.1. Pd–11.5 at.% Gd and Pd–14.0 at.% Gd alloys

Figures 4(*a*) and 4(*b*) show the electron diffraction patterns of the Pd–11.5 at.% Gd alloy which was exposed to a hydrogen pressure of 30 bar at 863 K and figure 4(*c*) the electron diffraction pattern of the Pd–14.0 at.% Gd alloy which was exposed to a hydrogen pressure of 30 bar at 903 K; these temperatures are above the peritectoid temperatures. After the hydrogen exposures and cooling in hydrogen, the reflection spots at $(\frac{1}{2}\frac{1}{2}\frac{1}{2})$ which are characteristic of the Pd_7Gd superlattice appear to be split; this is unclear and weak in some regions (figures 4(*a*) and 4(*c*)) and, in other regions, the $L1_2$-type reflections, which are due to the Pd_3Gd phase (figure 4(*b*)) which coexists with the α-Pd phase, remain the same without any marked changes. The $L1_2$-type reflections for the Pd–14.0 at.% Gd alloy were more intense but are not given here. Thus, it can be seen that the peritectoid reaction of α-Pd + Pd_3Gd to Pd_7Gd in these alloys is suppressed by exposure to a hydrogen atmosphere and subsequent slow cooling to room temperature in hydrogen (about 30 bar).

Figures 5(*a*) and 5(*b*) show the diffraction patterns of the Pd–11.5 at.% Gd and Pd–14.0 at.% Gd alloys, respectively, hydrogen treated at 753 K for 1 h, the Pd–11.5 at.% Gd alloy was initially in the two-phase coexistence field of the α-Pd and Pd_7Gd phases, and the Pd–14.0 at.% Gd alloy was initially a two-phase mixtures of Pd_7Gd and Pd_3Gd phases.

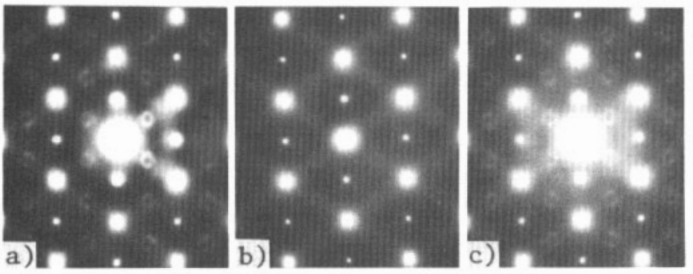

Figure 4. Electron diffraction patterns with [110] incidence for (*a*), (*b*) hydrogen-exposed Pd–11.5 at.% Gd and (*c*) hydrogen-exposed Pd–14.0 at.% Gd alloys, which were initially in the two-phase coexistence field of α-Pd + Pd_3Gd phases. The temperatures for hydrogen exposure (p_{H_2} = 30 bar for 1 h) were as follows: (*a*), (*b*), 863 K; (*c*) 903 K.

The Pd–11.5 at.% Gd alloy exhibits mainly diffraction patterns of the suppressed Pd_7Gd structure (figure 5(*a*)), and the Pd–14.0 at.% Gd alloy shows mainly only the patterns of the Pd_3Gd phase (figure 5(*b*)). Thus, the short-range-ordered Pd_7Gd phase coexisting initially with the α-Pd or Pd_3Gd phases has a tendency to disappear rather than to separate into two phases, after exposure to hydrogen.

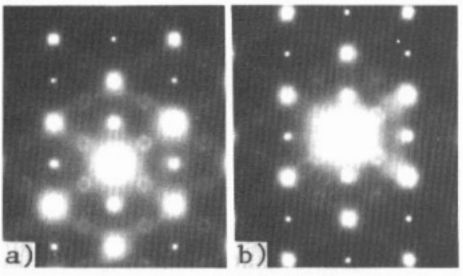

Figure 5. Electron diffraction patterns with [110] incidence for (*a*) hydrogen-exposed Pd–11.5 at.% Gd and (*b*) hydrogen-exposed Pd–14.0 at.% Gd alloys, where the former was initially in the two-phase coexistence field of α-Pd + Pd_7Gd phases, and the latter was a two-phase mixture of Pd_7Gd + Pd_3Gd phases. The temperature for the hydrogen exposure (p_{H_2} = 30 bar for 1 h) was 753 K.

The suppression of the peritectoid reaction in the presence of hydrogen during cooling of the alloys, and the disordering of short-range-ordered Pd_7Gd phase initially coexisting with a α-Pd or Pd_3Gd phases seems to be related to the preferential occupancy by hydrogen of octahedral interstices surrounded entirely by nearest-neighbour Pd atoms in the α-Pd or Pd_7Gd phases because the diffraction patterns of the coexisting Pd_3Gd phase do not undergo any substantial changes on hydrogen exposure. The hydrogen solubility in the Pd_3Gd phase is expected to be much less than in the more Pd-rich α-Pd and short-range-ordered Pd_7Gd phases. The preferential occupancy of hydrogen by α-Pd or Pd_7Gd phases may consequently act to weaken the Pd–Gd attractive interaction which leads to ordering.

In order to examine the reverse transformation from the state resulting from exposure and cooling in hydrogen to the original state, the cooled alloys were heated *in vacuo*, and

electrical resistance measurements were carried during the heating and subsequent cooling at a rate of 50 K h^{-1}. An electrical resistance versus temperature relationship for the initially hydrogen-containing Pd–11.5 at.% Gd alloy is shown in figure 6 in comparison with that of the 'hydrogen-free' as-quenched sample [1].

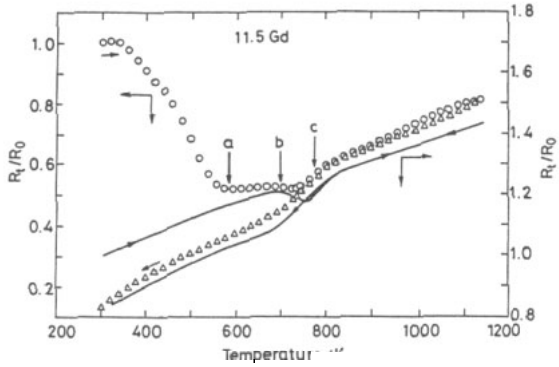

Figure 6. Electrical resistance versus temperature relationships for the initially hydrogen-containing Pd–11.5 at.% Gd alloy resulting from treatment for 1 h at 863 K with $p_{H_2} = 30$ bar and then cooling in hydrogen: ○, subsequent heating *in vacuo*; △, subsequent cooling *in vacuo* at a rate of 50 K h^{-1}; ——, 'hydrogen-free' as-quenched alloy [1]; the arrows on the heating curve indicate the temperatures at which the samples for electron diffraction were quenched and analysed.

Figure 7 shows the variation in the electron diffraction patterns of the Pd_7Gd superlattice in the Pd–11.5 at.% Gd alloy, as the initial as-hydrogen-treated samples were heated and then quenched from the following temperatures according to the data on the resistance measurements (figure 6) : figure 7(*a*), 583 K; figure 7(*b*), 693 K; figure 7(*c*) 773 K.

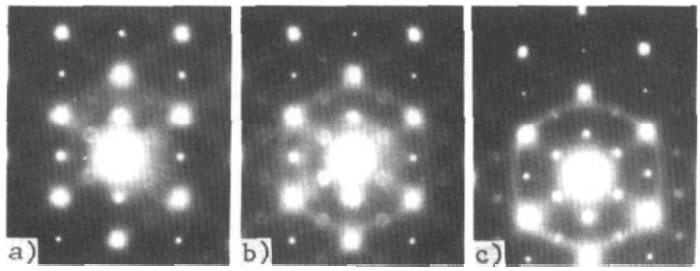

Figure 7. Electron diffraction patterns with [110] incidence for Pd–11.5 at.% Gd alloy, as the initially hydrogen treated samples were heated and quenched from (*a*) 583 K, (*b*) 693 K and (*c*) 773 K (see figure 6).

Following a rapid decrease in resistance to about 573 K due to the loss of the hydrogen introduced during the hydrogen treatment, the resistance then remains almost constant on further heating and then a small decrease in resistance occurs at about 723 K owing to the commencement of ordering to Pd_7Gd (figures 7(*b*) and 7(*c*)). Upon further heating, the ordered phase starts to disorder, leading to the coexistence of the α-Pd and Pd_3Gd phases.

3.2. Pd–11.5 at.% Sm and Pd–13.7 at.% Sm alloys

Electron diffraction patterns of the Pd–11.5 at.% Sm and the Pd–13.7 at.% Sm alloys exposed to hydrogen at 873 K and 913 K, respectively, which were initially in the two-phase coexistence field of α-Pd + H-Pd_5Sm phases, show that, in addition to the existence of the hydrogen-induced suppressed Pd_7Sm structure, some regions exhibit $L1_2$-type reflections due to the Pd_3Sm phase. Figure 8 shows an example of the diffraction patterns for the hydrogen-exposed Pd–11.5 at.% Sm alloy; figure 8(a) is the pattern of the suppressed Pd_7Sm structure, and figure 8(b) is that of $L1_2$-type Pd_3Sm. Thus, it can be seen that a system in the H-Pd_5Sm+α-Pd two-phase field above the peritectoid reaction temperature transforms to the Pd_3Sm structure under the action of hydrogen, i.e. H-$Pd_5SmH_x \rightarrow Pd_3Sm + 2PdH_y$, where $x = 2y$.

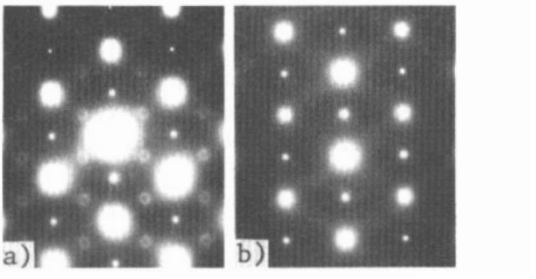

Figure 8. Electron diffraction patterns with [110] incidence for hydrogen-exposed Pd–11.5 at.% Sm alloy, which was initially in the two-phase coexistence field of α-Pd + H-Pd_5Sm phases. The temperature for hydrogen exposure (p_{H_2} = 30 bar for 1 h) was 873 K.

Even if these alloys were exposed to hydrogen at temperatures below the peritectoid reaction temperature, e.g. at 673 and 753 K, $L1_2$-type reflections are observed in the samples, together with that of the suppressed Pd_7Sm structure; in the case of exposure to hydrogen of the hyperperitectoid Pd–13.7 at.% Sm alloy at 673 K the reflections due to the Pd_7Sm were relatively strong and clear. As described for the formation of the $L1_2$-type Pd_3Sm superlattice above, if the Pd_3Sm really forms from exposure of the H-Pd_5Sm phase to hydrogen, the Pd_5Sm phase should not exist in the Pd–11.5 at.% Sm alloy which is a hypoperitectoid composition according to the equilibrium phase diagram [2]. However, the existence of the Pd_3Sm phase in the hydrogen-exposed Pd–11.5 at.% Sm alloy is clear. This, as has been discussed [2], implies that in the absence of hydrogen the peritectoid reaction takes a long time to reach complete equilibrium in these alloys. Figure 9(a) shows an example of the diffraction pattern of the Pd–11.5 at.% Sm alloy and figures 9(b) and 9(c) the diffraction patterns of the Pd–13.7 at.% Sm alloy which were hydrogen treated at 673 K; figure 9(a) is the pattern of the suppressed Pd_7Sm, figure 9(b) is a relatively clear pattern of the Pd_7Sm structure and figure 9(c) is the pattern of the transformed $L1_2$-type Pd_3Sm.

Figures 10(a) and 10(b) show the results of electrical resistance versus temperature relationships for initially hydrogenated Pd–11.5 at.% Sm and Pd–13.7 at.% Sm alloys, respectively, in comparison with that of 'hydrogen-free' as-quenched samples [2]. A small decrease in resistance at about 780 K for the Pd–11.5 at.% Sm alloy and at about 800 K for the Pd–13.7 at.% Sm alloy, can also be seen; these decreases are due to ordering from the suppressed Pd_7Sm structure and the transformed Pd_3Sm to the Pd_7Sm phase. On further

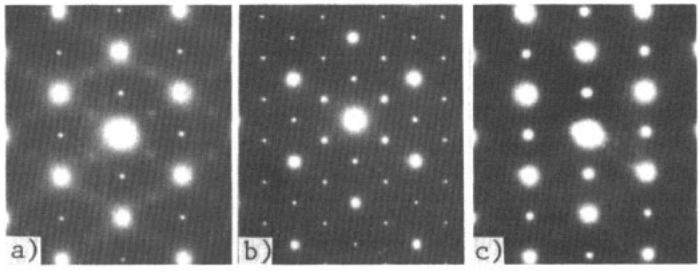

Figure 9. Electron diffraction patterns with [110] incidence for (*a*) hydrogen-exposed Pd–11.5 at.% Sm and (*b*), (*c*) hydrogen-exposed Pd–13.7 at.% Sm alloys, where the former was initially in the two-phase coexistence field of α-Pd + Pd_7Sm phases, and the latter was a two-phase mixture of Pd_7Sm + H-Pd_5Sm phases. The temperature for the hydrogen exposure (p_{H_2} = 30 bar for 1 h) was 673 K.

heating, an abrupt decrease in resistance appears at about 860 K for both alloys owing to the transition back to the H-Pd_5Sm and α-Pd phases. Figure 11 shows the diffraction patterns for the Pd–13.7 at.% Sm alloys, as the initial hydrogen-exposed samples were heated and then quenched for analysis from the following temperatures according to the resistance data (figure 10(*b*)) : figure 11(*a*), 619 K; figures 11(*b*) and 11(*c*), 773 K; figure 11(*d*), 833 K; figure 11(*e*), 893 K.

The diffraction patterns of the Pd–11.5 at.% Sm alloy quenched from 619 K (figure 11(*a*)) and from 583 K (figure 10(*a*)) exhibit mainly reflections due to the $L1_2$-type Pd_3Sm and, in some regions of the samples quenched from 673 K, 723 K, 773 K (figures 11(*b*) and (*c*)), 793 K and 813 K, reflections are seen from Pd_3Sm, and other regions show reflections of the Pd_7Sm structure; the samples quenched from 833 K (figure 11(*d*)) exhibit mainly reflections of the Pd_7Sm structure. As can be seen from figure 11(*e*), however, the Pd_3Sm and Pd_7Sm phases are no longer seen for the Pd–13.7 at.% Sm alloy quenched from 893 K, and reflections characteristic of the H-Pd_5Sm structure [2] are mainly observed in addition to the fundamental reflections from the α-Pd phase.

It is of interest that the abrupt decrease in resistance appears on retransforming to the H-Pd_5Sm and α-Pd phases. This may be due to the existence of some still untransformed or remaining Pd_3Sm during the transition to the ordered Pd_7Sm phase e.g. some intermediate structures which remain up to the retransition to the H-Pd_5Sm + α-Pd phases. In fact, in some regions of the hydrogen-exposed samples, electron diffraction patterns considered to be rhombohedral $Pd_{17}Sm_2$ in the $[\bar{1}41]$ orientation [14] or rhombohedral Pd_7Sm_2 in the [100] orientation [14] were often observed, although there were some discrepancies compared with the calculated reflection spots, suggesting that the structures may be subject to small modifications of the atomic positions.

The formation of the $L1_2$-type Pd_3Sm from the H-Pd_5Sm phase by hydrogen exposure and the reverse transition of the Pd_3Sm to the H-Pd_5Sm phases by heating the samples *in vacuo* has also been confirmed by x-ray diffraction. Figure 12(*a*) shows the x-ray diffraction pattern of hydrogen-treated Pd–13.7 at.% Sm alloy, figure 12(*b*) the x-ray diffraction pattern of the same alloy heated at 773 K for 20 min and figure 12(*c*) the x-ray diffraction pattern of the same alloy heated at 893 K for 30 min. The hydrogen exposure was carried out at 913 K for 1 h with p_{H_2} = 30 bar and then quickly cooled at a rate of about 560 K h^{-1}, and not at about 50 K h^{-1} as described above. On the other hand, the heating treatments of the hydrogen-treated samples were carried out by inserting the alloys into the furnace which

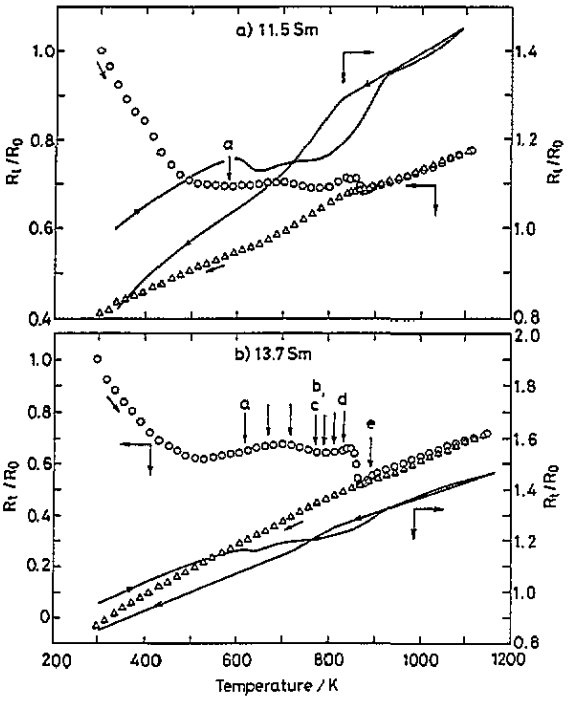

Figure 10. Electrical resistance versus temperature for the initially hydrogen-treated alloys of (*a*) Pd–11.5 at.% Sm at 873 K and (*b*) Pd–13.7 at.% Sm at 913 K with p_{H_2} = 30 bar for 1 h: ○, subsequent heating *in vacuo*; △, subsequent cooling *in vacuo* at a rate of 50 K h^{-1}; ——, 'hydrogen-free' as-quenched alloys [2]; the arrows on the heating curves indicate the temperatures at which the samples for electron diffraction were quenched and analysed.

had been controlled at the specified temperatures *in vacuo*. Before insertion of the alloys, argon gas was admitted into the furnace and then evacuated; after the specified heating time, the furnace was again replaced by argon gas and the samples were then rapidly quenched into ice–water.

The presence of the $L1_2$-type Pd_3Sm in the hydrogen-treated sample is confirmed and is stable during heating at 773 K for 20 mins *in vacuo* but, after heating the hydrogen-treated samples at 893 K for 30 min, the Pd_3Sm phase is transformed back into the H-Pd_5Sm phase. It should be noted here that, even if the hydrogen exposure is carried out by slow cooling at about 50 K h^{-1}, formation of the $L1_2$-type Pd_3Sm phase can be observed.

The mechanism of the transition of the H-Pd_5Sm to the $L1_2$-type Pd_3Sm phase is unknown but it must be a consequence of the lattice expansion accompanying the absorption of hydrogen in a specific set of lattice sites in the H-Pd_5Sm lattice, i.e. the lattice expansion may allow the necessary metal atom rearrangement.

3.3. Pd–10.0 at.% Eu, Pd–11.2 at.% Eu, Pd–12.2 at.% Eu, Pd–13.3 at.% Eu and Pd–14.3 at.% Eu alloys

Hydrogen treatment (p_{H_2} = 30 bar) of Pd–Eu alloys was carried out at temperatures above the peritectoid reaction for 1 h; the alloys are initially in the two-phase coexistence field of α-Pd + H-Pd_5Eu phases, i.e. at T = 893 K for Pd–10.0 at.% Eu, and at T = 933 K for the Pd–11.2 at.% Eu, Pd–12.2 at.% Eu, Pd–13.3 at.% Eu and Pd–14.3 at.% Eu alloys, but the

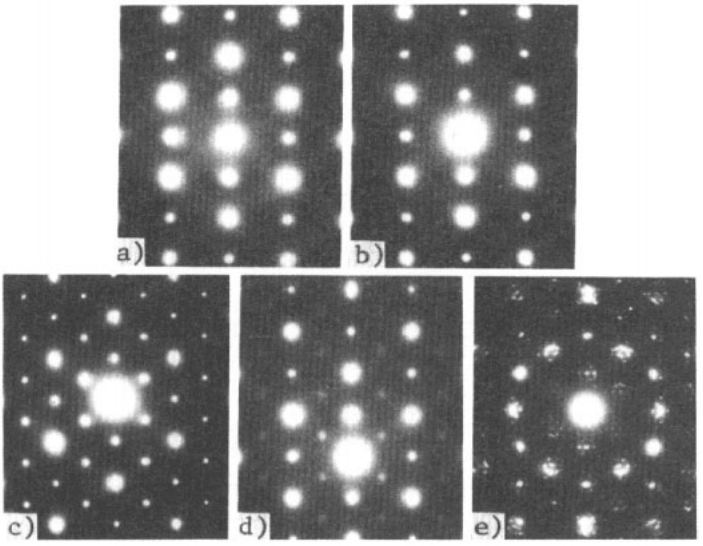

Figure 11. Electron diffraction patterns for Pd–13.7 at.% Sm alloys, as the initially hydrogen-exposed samples were heated and quenched from (*a*) 619 K, (*b*), (*c*) 773 K, (*d*) 833 K and (*e*) 893 K (see figure 10(*b*)). The beams are along [110] for (*a*)–(*d*), and along [001] for (*e*).

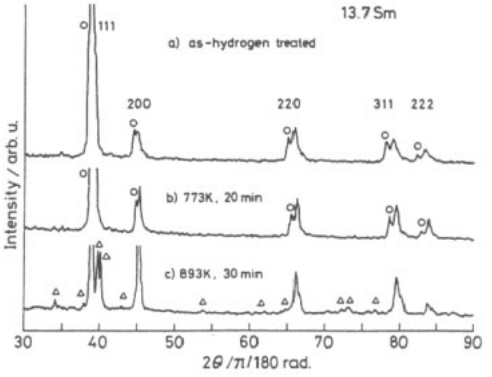

Figure 12. X-ray diffraction patterns of (*a*) as-hydrogen-exposed Pd–13.7 at.% Sm alloy, (*b*) the alloy quenched after heating at 773 K for 20 min *in vacuo* and (*c*) the alloy quenched after heating at 893 K for 30 min *in vacuo*: ○, $L1_2$-type Pd_3Sm; △, H-Pd_5Sm. Cu Kα radiation with a nickel filter was used.

Pd–10.0 at.% Eu alloy is almost on the solid solubility limit of europium in the α-Pd phase [3].

Electron diffraction patterns of all the hydrogen-exposed alloys exhibit, in addition to regions of hydrogen-suppressed Pd_7Eu structure, regions which have the $L1_2$-type reflections due to the Pd_3Eu phase, although the diffraction patterns for the Pd–10.0 at.% Eu alloy have only reflections due to the suppressed Pd_7Eu structure. Figure 13 shows an example of the diffraction patterns of hydrogen-exposed samples of Pd–11.2 at.% Eu alloy; figure 13(*a*) is the pattern of the suppressed Pd_7Eu structure, and figure 13(*b*) is the pattern of the $L1_2$-

type Pd_3Eu. Therefore, similar to the H-Pd_5Sm phase described above, it can be seen that the H-Pd_5Eu phase which initially coexists with the α-Pd phase above the peritectoid is transformed to the $L1_2$-type Pd_3Eu under hydrogen exposure.

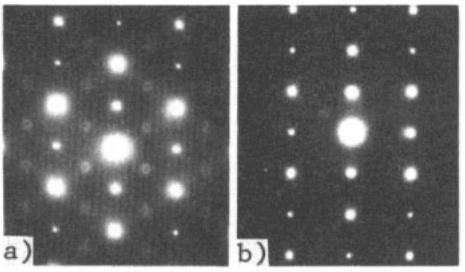

Figure 13. Electron diffraction patterns with [110] incidence for hydrogen-exposed Pd–11.2 at.% Eu alloys, which were initially in the two-phase coexistence field of α-Pd + H-Pd_5Eu phases. The temperature for hydrogen exposure (p_{H_2} = 30 bar for 1 h) was 933 K.

When the Pd–11.2 at.% Eu and Pd–14.3 at.% Eu alloys were exposed to hydrogen at 673 K, which is well below the peritectoid, the electron diffraction patterns exhibit mainly $L1_2$-type reflections although, for the hyperperitectoid Pd–14.3 at.% Eu alloy, relatively strong and clear reflections of the Pd_7Eu superlattice are observed. The formation of the $L1_2$-type Pd_3Eu phase is also due to the transition from the H-Pd_5Eu phase which coexists initially with the Pd_7Eu phase, although the Pd_5Eu should not also exist in the hypoperitectoid composition Pd–11.2 at.% Eu. This also implies that in the absence of hydrogen the peritectoid reaction requires a long time to reach complete equilibrium in these alloys [3]. Figures 14(*a*) and 14(*b*) show the diffraction patterns of the Pd_7Eu and of the transformed Pd_3Eu phases, respectively, in the Pd–14.3 at.% Eu alloy exposed to hydrogen at 673 K with p_{H_2} = 30 bar for 1 h.

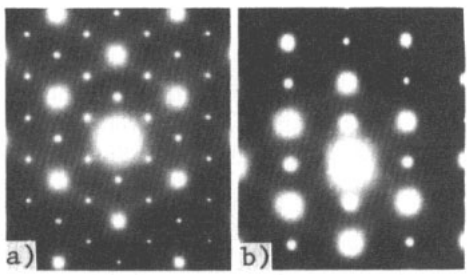

Figure 14. Electron diffraction patterns with [110] incidence for hydrogen-exposed Pd–14.3 at.% Eu alloy, which was initially in the two-phase coexistence field of Pd_7Eu + H-Pd_5Eu phases. The temperature for hydrogen exposure (p_{H_2} = 30 bar for 1 h) was 673 K.

Figure 15 shows the electrical resistance versus temperature for an initially hydrogen-treated Pd–13.3 at.% Eu alloy in comparison with that of a 'hydrogen-free' as-quenched sample [3]. During heating of the hydrogen-treated alloy, there is also a small decrease in

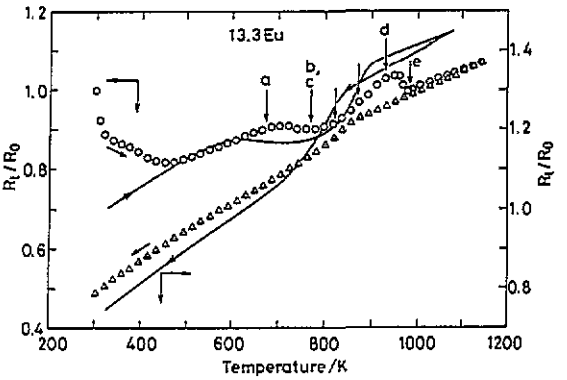

Figure 15. Electrical resistance versus temperature for the initially hydrogen-containing Pd–13.3 at.% Eu alloy resulting from treatment for 1 h at 933 K with p_{H_2} = 30 bar: ○, subsequent heating *in vacuo*; △, subsequent cooling *in vacuo* at a rate of 50 K h^{-1}; ——, 'hydrogen-free' as-quenched alloy [3]; the arrows on the heating curve indicate the temperatures at which the samples for electron diffraction were quenched and analysed.

resistance due to ordering from the suppressed Pd_7Eu structure and the transition from the Pd_3Eu phase to the Pd_7Eu phase, and also an abrupt decrease in resistance at about 980 K due to the retransition to the H-Pd_5Eu and α-Pd phases. Figure 16 shows the diffraction patterns for the Pd–13.3 at.% Eu alloy, as the initial as-hydrogen-treated alloy was heated and then quenched from the following temperatures: figure 16(*a*), 673 K; figures 16(*b*) and 16(*c*), 773 K; figure 16(*d*), 933 K; figure 16(*e*), 983 K. The diffraction patterns of the sample quenched from 673 K (figure 16(*a*)) exhibit mainly reflections due to $L1_2$-type Pd_3Eu; some regions of the samples quenched from 773 K (figures 16(*b*) and 16(*c*)), 823 K and 873 K show reflections due to the Pd_3Eu phase, and other regions show reflections of the Pd_7Eu structure; however, the samples quenched from 933 K (figure 16(*d*)) exhibit mainly the short-range-ordered Pd_7Eu phase. The patterns of some regions of samples quenched from 983 K (figure 16(*e*)) exhibit reflections due to the hexagonal Pd_5Eu phase, whereas other regions have only the fundamental reflections from the α-Pd solid solution.

As observed for hydrogen-treated Pd–Sm alloys (figures 10 and 11), the abrupt decrease in resistance related to the re-formation of the two-phase field (H-Pd_5Eu+α-Pd) may be due to the presence of some intermediate structures of Pd_3Eu coexisting with the Pd_7Eu phases directly up to the temperature for the retransition to the H-Pd_5Eu+α-Pd two-phase field. Similarly, for the Pd–Sm alloys, in some regions of the samples, electron diffraction patterns which were considered to be rhombohedral $Pd_{17}Eu_2$ in the $[\bar{1}4\bar{1}]$ orientation [14] or rhombohedral Pd_7Eu_2 in the [100] orientation [14] were often observed although the reflection spots did not lie exactly as in the calculated patterns.

In a similar way to that described for the hydrogen-treated Pd–13.7 at.% Sm alloy, the formation of Pd_3Eu from the H-Pd_5Eu phase by hydrogen exposure was confirmed by x-ray diffraction analysis, and the reverse transition of the Pd_3Eu to H-Pd_5Eu phases by heating the samples *in vacuo* was confirmed similarly.

Figures 17(*a*), 17(*b*) and 17(*c*) show the x-ray diffraction pattern of hydrogen-treated Pd–14.3 at.% Eu alloy, of the alloy heated at 773 K for 20 min and of the alloy heated at 1003 K for 30 min, respectively. The hydrogen exposure was carried out at 933 K for 1 h with p_{H_2} = 30 bar, and then the alloy was quickly cooled to room temperature at a rate of about 560 K h^{-1}. It can be seen that the $L1_2$-type Pd_3Eu phase formed by hydrogen

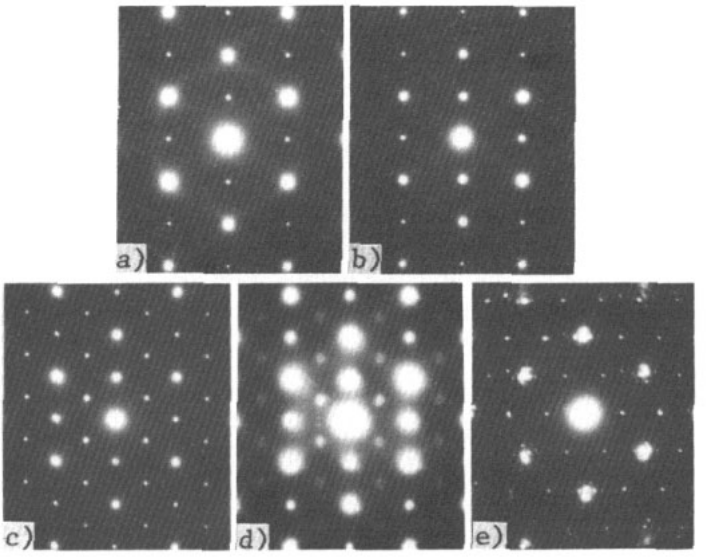

Figure 16. Electron diffraction patterns for Pd–13.3 at.% Eu alloy, as the initially hydrogen-exposed samples were heated and quenched from (*a*) 673 K, (*b*), (*c*) 773 K, (*d*) 933 K and (*e*) 983 K (see figure 15). The incident beams are along [110] for (*a*)–(*d*), and along [011] for (*e*).

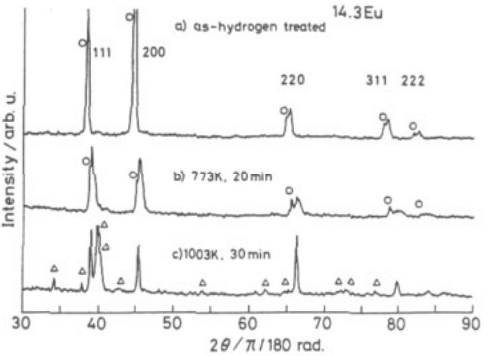

Figure 17. *X-ray diffraction pattern of (a) as-hydrogen-treated* Pd–14.3 at.% Eu alloy, (*b*) the alloy quenched after heating at 773 K for 20 min *in vacuo* and (*c*) the alloy quenched after heating at 1003 K for 30 min *in vacuo*: ○, $L1_2$-type Pd_3Eu; △, H-Pd_5Eu. Cu Kα radiation with a nickel filter was used.

exposure is also stable during heating at 773 K for 20 min *in vacuo*, but by heating at 1003 K for 30 min the Pd_3Eu phase is transformed back to the H-Pd_5Eu phase.

4. Conclusions

From the above results it can be concluded that the peritectoid reaction of α-Pd + Pd_3Gd (or H-Pd_5RE (RE ≡ Sm or Eu)) to Pd_7RE is suppressed by the presence of dissolved hydrogen introduced at temperatures above the peritectoid reaction temperature and then cooled below

it with dissolved hydrogen. For the Pd–Gd alloys, the suppression of ordering to Pd_7Gd is suggested to be due to the retardation of nucleation and growth of the Pd_7Gd ordered domain as a consequence of weakening of the Pd–Gd bonding by the dissolved hydrogen in the α-Pd phase. For the Pd–Sm and Pd–Eu alloys, the suppression is related to the transition of the initially coexisting H-$Pd_5Sm(Eu)$+α-Pd phases to the $L1_2$-type $Pd_3Sm(Eu)$ phase under a hydrogen atmosphere. Similarly, the presence of interstitial hydrogen has the tendency to eliminate the short-range-ordered $Pd_7Gd(Sm, Eu)$ phases which coexist with the α-Pd, Pd_3Gd and/or H-$Pd_5Sm(Eu)$ phases below the peritectoid reaction temperatures. Furthermore, for the low-temperature hydrogen exposures, the $Pd_5Sm(Eu)$ phase which coexists initially with the $Pd_7Sm(Eu)$ phase transforms to the $L1_2$-type $Pd_3Sm(Eu)$ phase.

References

[1] Sakamoto Y, Takao K, Yoshida M and Flanagan T B 1988 *J. Less-Common Met.* **143** 207
[2] Sakamoto Y, Takao K, Takeda S and Takeda T 1989 *J. Less-Common Met.* **152** 127
[3] Takao K, Zhao K L and Sakamoto Y 1990 *J. Mater Sci.* **25** 1255
[4] Schneider A and Esch U 1944 *Z. Elektrochem.* **50** 290
[5] Sakamoto Y, Takao K, and Flanagan T B 1993 *J. Phys.: Condens. Matter* **5** 4171
[6] Salomons E, Koeman N, Rector J and Griessen R 1990 *J. Phys.: Condens. Matter* **2** 835
[7] Doyle M L, Wileman R C J and Harris I R 1987 *J. Less-Common Met.* **130** 79
[8] Kuwano N, Shiwaku T, Tomokiyo Y and Eguchi T 1981 *Japan. J. Appl. Phys.* **20** 1603
[9] Smith D A, Jones I P and Harris I R 1982 *J. Mater. Sci. Lett.* **1** 463
[10] Haucke W 1940 *Z. Anorg. (Allg.) Chem.* **244** 17
[11] Heumann Th. and Kniepmeyer M 1950 *Z. Anorg. (Allg.) Chem.* **290** 191
[12] Kuwano N, Hiroshige I, Tomokiyo Y and Eguchi T 1983 *Proc. of 7th Int. Conf. on High Voltage Electron Microscopy (Berkeley, CA 1983)* p 291
[13] Itakura M, Hisatsune Y, Sato H, Kuwano N and Oki K 1988 *Japan. J. Appl. Phys.* **27** 684
[14] Rao P and Goehner R P 1974 *J. Appl. Crystallogr.* **7** 482
[15] Takeda S, Horikoshi H and Komura Y 1983 *J. Microsc.* **129** 347